

SL20

KUMULANTY V PROFILOVÉ ANALÝZE

M. Čerňanský

*Fyzikální ústav AV ČR, v.v.i., Na Slovance 2, 182 21 Praha 8, Česká republika
cernan@fzu.cz*

Kumulanty, resp. semiinvarianty jsou po momentech dalším pojmem z teorie pravděpodobnosti a matematické statistiky, které lze výhodně využít při analýze profilů difrakčních linií. Obvykle se definují následujícím způsobem.

Označme $f(x)$ jako hustotu (rozložení) pravděpodobnosti náhodné proměnné x . Jinými slovy, pravděpodobnost toho, že náhodná proměnná x je z intervalu $(x, x + dx)$ je $f(x)dx$ a zřejmě platí podmínka pro normování pravděpodobnosti

$$\int_{-\infty}^{\infty} f(x)dx = 1 \quad (1)$$

K hustotě pravděpodobnosti $f(x)$ se v případě spojité náhodné proměnné x definuje, např. [1, 2], pravděpodobnostní vytvořující funkce $G(t) = G(t; f)$ vztahem

$$G(t) = \int_{-\infty}^{\infty} f(x)t^x dx \quad (2)$$

Položíme-li v (2) $t = e^a$, obdržíme momentovou vytvořující funkci

$$G(e^a) = \int_{-\infty}^{\infty} f(x)\exp(ax)dx = 1 + m_1 a + \frac{m_2 a^2}{2!} + \frac{m_3 a^3}{3!} + \dots = M(a) \quad (3)$$

a rozvojem logaritmu momentové vytvořující funkce $M(a)$ dostáváme vytvořující funkci kumulantů

$$K(a) = \ln M(a) = 1 + \frac{1}{1} a + \frac{1}{2} a^2 + \frac{1}{3} a^3 + \dots, \quad (4)$$

kde m_n jsou kumulanty hustoty pravděpodobnosti $f(x)$.

V praxi se většinou kumulanty počítají z momentů pomocí rekurentního vztahu

$$m_n = \frac{n-1}{n} m_{n-1} + \frac{1}{n} m_{n-2} m_2 + \dots + \frac{1}{n} m_{n-k} m_k, \quad (5)$$

kde m_n jsou momenty kolem počátku

$$m_n = \int_{-\infty}^{\infty} x^n f(x)dx, \quad n = 0, 1, \dots \quad (6)$$

Číslo n je řád momentu nebo kumulantu. Speciálně $m_1 = m_1$, t.j. první kumulant je roven těžišti rozložení $f(x)$. Pro další kumulanty pak z (5) vychází

$$m_2 = m_2, \quad (7)$$

$$m_3 = m_3 - 3m_2 m_1, \quad (8)$$

$$m_4 = m_4 - 4m_3 m_1 - 3m_2^2, \quad (9)$$

$$m_4 = m_4 - 4m_1 m_3 - 3(m_2)^2 - 12m_2(m_1)^2 - 6(m_1)^4, \quad (10)$$

Vztahy pro výpočet kumulantů z centrálních momentů

$$m_n = \int_{-\infty}^{\infty} (x - m_1)^n f(x)dx, \quad n = 0, 1, \dots \quad (11)$$

jsou zřetelně jednodušší

$$m_2 = \sigma^2, \quad (12)$$

$$m_3 = 3\sigma^3 \gamma_1, \quad (13)$$

$$m_4 = 3\sigma^4 (\gamma_2 + 3\gamma_1^2), \quad (14)$$

a vidíme, že druhý kumulant je roven varianci funkce $f(x)$.

Při analýze difrakčních profilů jsou nejužitečnější ty vlastnosti kumulantů, které souvisí s konvolucí. Je známo, že těžiště konvoluce $h = f * g$ je součtem těžišť funkcí f a g a totéž platí pro variance [3]. Stejně jednoduchý vztah platí ještě pro třetí centrální momenty, ale pro momenty vyšších řádů platí složitější vztah [4]

$$m_{n,h} = \sum_{k=0}^n \binom{n}{k} m_{n-k,f} m_{k,g}, \quad (15)$$

Naproti tomu pro kumulanty funkcí v konvoluci $h = f * g$ platí pro všechny řády n [1, 5]

$$m_{n,h} = m_{n,f} + m_{n,g}, \quad (16)$$

Dále mají kumulanty velmi cennou vlastnost u vícenásobné konvoluce $h = p * q * r * s * t \dots$ [5]

$$m_{n,h} = m_{n,p} + m_{n,q} + m_{n,r} + m_{n,s} + m_{n,t} + \dots, \quad (17)$$

kteřá byla navržena k analýze kombinace jednotlivých geometrických aberací způsobených nedokonalostí přístroje [6].

Kumulanty byly použity rovněž při interpretaci fyzikálních profilů [7], zejména při analýze metody čtvrtých momentů na určení velikosti krystalitů a mikrodeformací z jedné linie [8-10].

Ze snadno vypočtených kumulantů lze přímo nebo pomocí momentů vypočíst hledanou funkci, např. fyzikální profil f . K tomu lze použít vztahy [11, 12] inverzní k rovnicím typu (14)

$$m_4 = m_4 - 3m_2^2 - 6m_1^4, \quad (18)$$

a pak použít např. Edgeworthovu řadu [7, 11], nebo Grammovu-Charlierovu řadu [7, 12], přičemž počet



členů může být malý. Zpravidla stačí rozvoj do čtvrtého momentu [11].

1. A.C. Aitken: *Statistical Mathematics*. Edinburgh and London 1947. Oliver and Boyd.
2. J. Hátle & J. Kahounová: *Úvod do teorie pravděpodobnosti*. Praha 1987. SNTL/Alfa.
3. A.J.C. Wilson: *Mathematical Theory of X-Ray Powder Diffractometry*. Eindhoven 1963. Philips Technical Library.
4. A. Fingerland: *Czech J. Phys. B* 10 (1960) 233-239.
5. L. Janossy: *Theory and Practice of the Evaluation of Measurements*. Oxford 1965. Oxford University Press.
6. A.J.C. Wilson: *J. Appl. Cryst.* 6 (1973) 230-237.

7. M. Čerňanský: *Z. Kristallogr.* v tisku.
8. A.S. Kagan & V.M. Snovidov, *Fizika metallov i metallovedeniye*, 19 (1965) 191-198.
9. V.M. Snovidov, A.S. Kagan & A.E. Kovalskii: *Zav. Lab.* 34 (1968) 1086-1088.
10. J. Neumann & M. Čermák, *Čs. čas. fyz. A* 27 (1977) 601-603.
11. H. Cramér: *Mathematical Methods of Statistics*. Princeton 1946. Princeton University Press
12. M.G. Kendall & A. Stuart: *The Advanced Theory of Statistics*, Vol. 1. London 1969. Charles Griffin.

Tato práce vznikla v rámci realizace projektu Grantové agentury České republiky, číslo 106/07/0805.

SL21

SURFACE LAYERS STUDY OF BULKY SAMPLES BY X'PERT PRO DIFFRACTOMETER

Z. Pala¹, N. Ganev¹, J. Drahokoupil²

¹*Department of Solid State Engineering, Faculty of Nuclear Sciences and Physical Engineering, Czech Technical University in Prague, Trojanova 13, 120 00 Prague*

²*Institute of Physics of the ASCR, v. v. i., Na Slovance 2, 182 21 Prague
zdenek.pala@fffi.cvut.cz*

Samples for investigation by means of X-ray diffraction are frequently prepared solely and, therefore, suitably for the experimental arrangement, which often imposes stringent conditions to its shape, mass and dimensions. However, real samples from industrial production cannot be usually cut into feasible parts without changing their structural and physical properties. Generally, samples' amendments can even lead to redistribution of residual stresses by inducing new plastic deformations. Consecutive inspection of such artificially created objects has only limited relevance to the original state which is the centre of interest.

The appropriate attitude to XRD measurements of bulky and heavy samples is, first of all, a choice of convenient goniometer geometry. The theta-theta goniometer configuration offers comparatively large space for sample handling. Preferably, the sample mounting should be external and, thus, allowing placement of large volume beneath the investigated surface. Such external mounting stages should have large travel range with smallest possible position resolution and reading accuracy in both vertical and horizontal directions. Consequently, sufficiently precise position control cannot be omitted. This can be done by a high precision laser sensor for dimensional measurement which has ample resolution up to 0.001 mm.

In the experiment, three types of machined surface layers for guide gibs of dimensions $160 \times 105 \times 45 \text{ mm}^3$ were examined. Samples from the steel 11 375.0 were machined by milling, grinding, and scraping. Semiproducts were cut from the steel sheet without any heat treatment by using an acetylene jig-burner. The aim of the research was to characterize each surface by state of macroscopic residual stress on the very surface and in near surface area of ca 200 μm in depth. Moreover, profiles of diffraction line $\{211\}$

of $\alpha\text{-Fe}$ phase were used for calculation of microstrains and domains of coherent scattering by the single line Voigt function method [1]. Microhardness and metallographic measurements provide a supplement to diffraction results.

Sample positioning in the X'Pert PRO diffractometer is depicted in Fig. 1. A set of motorized and manual vertical and horizontal stages by *Standa* [2] was used for sample setting-up. Because the laser sensor was not available, mounting to the desired position was performed by a simple and straightforward alignment procedure recommended by *PANALYTICAL*. Its basic principle lies in a flat



Figure 1. Mounting of a guide gib for residual stress measurement by X'Pert PRO.

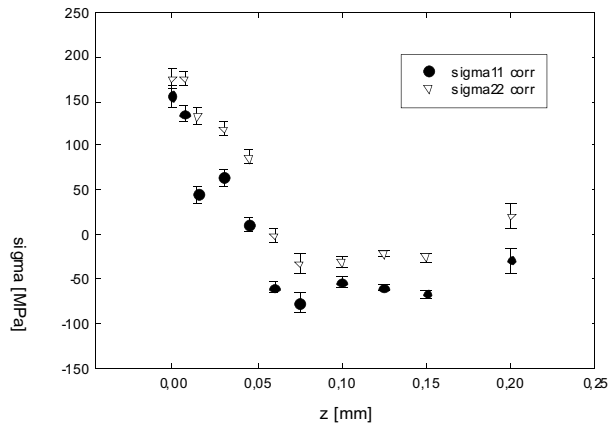


Figure 2a. Residual stress distribution in milled surface.

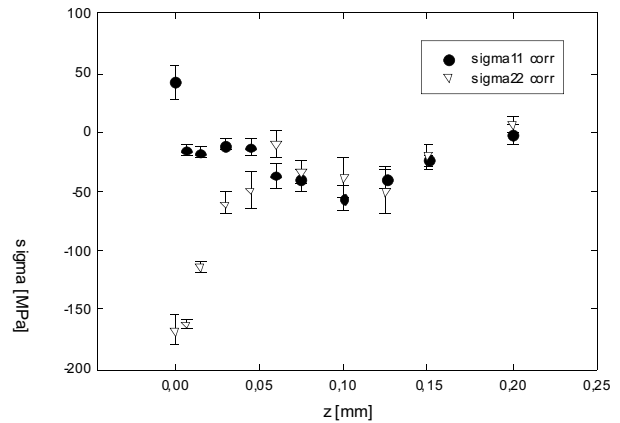


Figure 2b. Residual stress distribution in ground surface.

surface positioning to the level when it intersects the incident beam into two equivalent halves [3] which can be verified either by a suitable gauge or by intensity measurement.

State of biaxial macroscopic residual stress (RS) (Fig. 2) on the surface was established on three chosen areas of each sample in order to find out, in the first approximation, level of RS homogeneity in final surface. RS depth distribution was obtained by successive layer removal by electro-chemical polishing. Sets of diffraction data were evaluated by centre of gravity algorithm and biaxial state was assumed, shear stress was recorded only in ground surface. Results of RS after layer removal were corrected according to Moore and Ewans method [4].

1. Th. H. de Keijser, J. I. Langford, E. J. Mittemeijer, A. B. P. Vogels, *J. Appl. Cryst.*, **15**, (1982), 308.
2. www.standa.lt.
3. X'Pert PRO User's Guide, Fourth Edition, 2002.
4. Sikarskie D., *Trans. of the Metallurgical Society of AIME*. **239** (1967) 577–580.

The research was supported by the Project MSM q 6840770021 and by the Project q FT-TA4/105 of the Ministry of Industry and Trade of the Czech Republic.

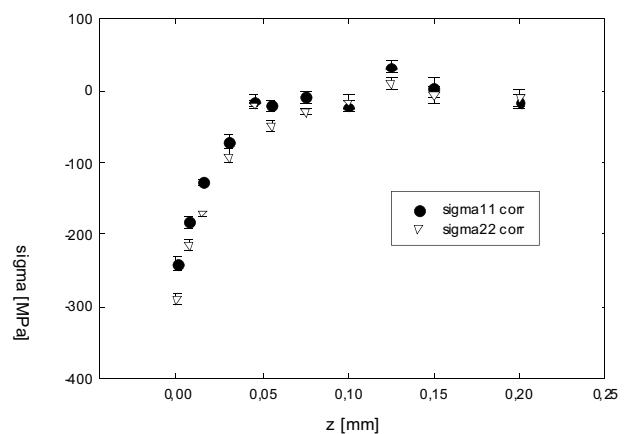


Figure 2c. Residual stress distribution in scraped surface.



SL22

COPLANAR GRAZING EXIT X-RAY DIFFRACTION ON THIN POLYCRYSTALLINE FILMS

Zdeněk Matěj, Lea Nichtová, Radomír Kužel

Charles University, Faculty of Mathematics and Physics, Ke Karlovu 3, Prague 12116, Czech Republic

X-ray powder diffraction analysis of thin polycrystalline films in the coplanar grazing exit (GE) parallel beam geometry was tested. Dependence of the diffraction peak intensity on the beam incidence/exit angle, which cannot be interpreted by a simple formula for absorption in the film [1], was observed for very thin films ($\ll 100$ nm for TiO_2). This effect is connected with the well known Yoneda peak in the transparency of the film surface interface. The refraction correction of peak positions and penetration depth [2], and also dynamical effects of multiple scattering of primary/diffracted beam in the film [3] should be considered. In comparison with the common coplanar grazing incidence geometry, by GE technique lower intensity gain for thin film can be achieved. However, if the PSD detector is used, 2D maps of scattered intensity with high resolution (because of narrow diffracted beam) can be obtained in a reasonable time. Moreover, they are not affected significantly by instrumental and sample effects. The technique is very useful for determination of the film thickness, depth profiling of phase composition, the refraction index determination and generally for study of real structure of thin films and multilayers with common laboratory diffractometers.

1. J. Lhotka, R. Kuzel, G. Cappuccio, V. Valvoda, *Surf. Coat. Tech.* (2001) **148**, 96-101.

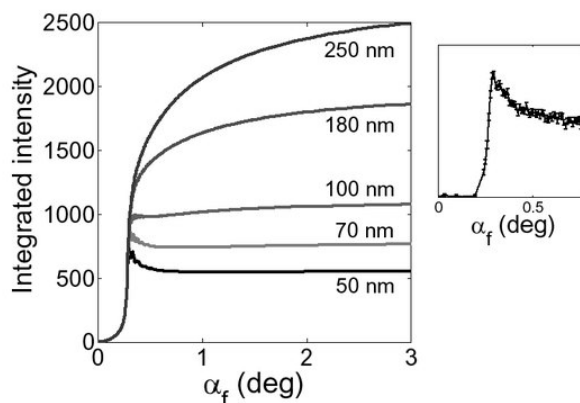


Figure 1. Simulated dependence of the integrated intensity of anatase (101) diffraction line on the exit angle α_f , for powder TiO_2 films of different film thickness. Measured intensity for the thinnest film (50 nm) is depicted in the right plot.

2. G. Lim, W. Parrish, C. Ortiz, M. Bellotto, M. Hart, *J. Mater. Res.* (1987) **2** (4) 471-477.
3. P. F. Fewster, N. L. Andrew, V. Holy, K. Barmak, *Phys. Rev. B* (2005) **72**, 174105.

SL23

IN-SITU XRD STUDY OF CRYSTALLIZATION OF AMORPHOUS TiO_2 THIN FILMS OF DIFFERENT THICKNESS

Lea Nichtová¹, Radomír Kužel¹, Zdeněk Matěj¹, Jan Šícha²

¹Department of Condensed Matter Physics, Faculty of Mathematics and Physics, Charles University in Prague, Ke Karlovu 5, 121 16 Praha 2

²Department of Physics, Faculty of Applied Sciences, University of West Bohemia in Pilsen, Czech Republic

Titanium dioxide films have found many different applications because of several excellent properties. First of all, this is photocatalytic activity and hydrophilicity after irradiation by UV radiation. Moreover, they are chemically stable and can have reasonably high hardness.

However, these properties depend significantly on the crystallinity, phase composition and microstructure of the films. In this study, crystallization of amorphous films with different thickness (50-2000 nm) deposited on silicon substrates was investigated by in-situ isochronal and isothermal annealing at different temperatures and compared with the post-annealing of both amorphous and nanocrystalline films.

The X'Pert Pro diffractometer with MRI high-temperature chamber and parallel beam geometry with Goebel mirror, for texture and stress measurements, the Eulerian cradle and polycapillary were used, respectively.

In earlier experiments, crystallization temperature of about 250 °C was found for thicker films while it was somewhat higher for very thin films (below 200 nm) [1, 2].

Therefore in-situ measurements were performed at slightly lower temperatures (180 °C, 220 °C) and time dependences of selected XRD profiles were investigated. It was found, that the process can well be described by the modified Avrami equation (see Fig. 1) that is applied to integrated intensities of the diffraction peaks,

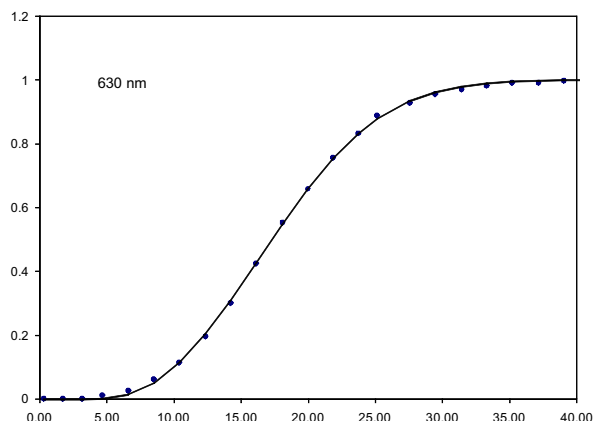


Figure 1. Normalized integrated intensity of anatase diffraction peak 101 in dependence on annealing time for the 630 nm thick film, dots - experimental data, line - fitted modified Avrami equation.

$$I = 1 - \exp[-b(t-t_0)^n],$$

where the exponent n was in the range 2–2.5 and it was slightly increasing with the film thickness. This lower value may indicate two dimensional character of the crystallite growth. The initial time t_0 of crystallization (non-zero intensity) increases nearly exponentially with the decreasing thickness while the slope b increases significantly for thicker films. Typical time necessary for the crystallization of the whole film volume varied from several hours for thicker layers to about ten days for the thinnest films, for

the used temperatures. Measurements confirmed that the crystallization of very thin films is rather slow (Fig. 2).

Fast crystallization of the order of minutes appeared at 230 °C for thicker films and was higher (290 °C) for the thin films with the thickness below 100 nm. This only confirmed the results obtained on post-annealed films.

Weak texture was changing during the crystallization since the intensity ratios of different peaks were varied with annealing time. At the beginning, the crystallites with the (001) orientation were developed. However, after complete crystallization, the texture was weak except the very thin films (below 100 nm).

Significant shifts of diffraction peaks with the temperature were observed and tensile residual stresses were confirmed by the \sin^2 method for different diffraction peaks. They decrease with the increasing film thickness. Line profile analysis indicated the growth of relatively large crystallites (100 nm) already at the beginning of crystallization unlike the films which were deposited as nanocrystalline with the crystallite size of 5–10 nm which remained nanocrystalline to relatively high temperatures (600 °C).

The work is supported by the Grant Agency of the Czech Republic (no. 106/06/0327) and Grant Agency of Charles University.

1. R. Kužel, L. Nichtová, D. Heřman, J. Šícha, J. Musil Growth of magnetron sputtered TiO₂ thin films studied by X-ray scattering, *Zeitschrift fuer Kristallographie. Suppl.* **26** (2007) 241-246.
2. R. Kužel, L. Nichtová, Z. Matěj, D. Heřman, J. Šícha, J. Musil, Study of crystallization of magnetron sputtered TiO₂ thin films by X-ray scattering, *Zeitschrift fuer Kristallographie. Suppl.* **26** (2007) 247-252.

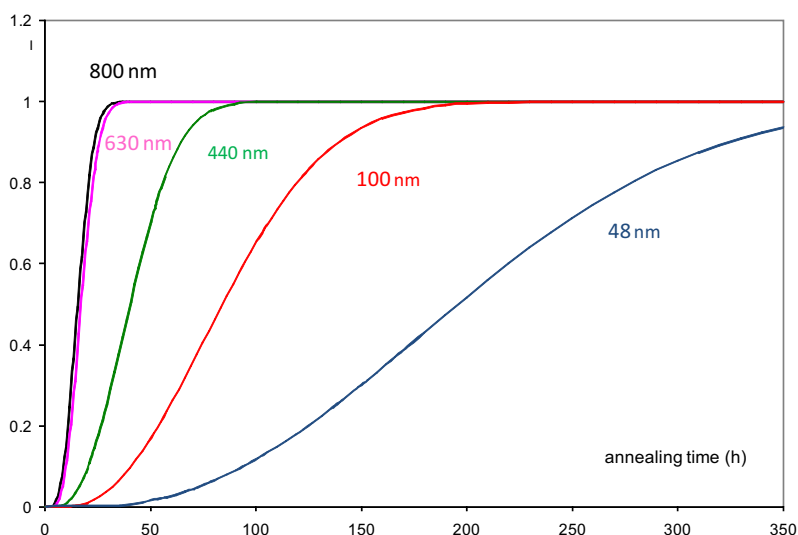


Figure 2. Normalized integrated intensity of anatase diffraction peak 101 in dependence on annealing time (annealing temperature 180 °C) for films of different thickness. Values were calculated by modified Avrami equation with the parameters fitted on experimental curves (Fig. 1). The thinnest film (48 nm) was heated to 220 °C.